

Association of Psb28 and Psb27 Proteins with PSII-PSI Supercomplexes upon Exposure of *Synechocystis* sp. PCC 6803 to High Light

Martina Bečková^{1,2}, Zdenko Gardian^{2,3}, Jianfeng Yu⁴, Peter Konik^{1,2}, Peter J. Nixon⁴ and Josef Komenda^{1,2,*}

¹Institute of Microbiology, Center Algatech, Opatovický mlýn, 37981 Třeboň, Czech Republic

²Faculty of Science, University of South Bohemia, Branišovská 1760, 37005 České Budějovice, Czech Republic

³Institute of Plant Molecular Biology, Biology Centre Academy of Sciences, Branišovská 31, 37005 České Budějovice, Czech Republic

⁴Sir Ernst Chain Building-Wolfson Laboratories, Department of Life Sciences, Imperial College London, South Kensington Campus, London SW7 2AZ, UK

*Correspondence: Josef Komenda (komenda@alga.cz)

<http://dx.doi.org/10.1016/j.molp.2016.08.001>

ABSTRACT

Formation of the multi-subunit oxygen-evolving photosystem II (PSII) complex involves a number of auxiliary protein factors. In this study we compared the localization and possible function of two homologous PSII assembly factors, Psb28-1 and Psb28-2, from the cyanobacterium *Synechocystis* sp. PCC 6803. We demonstrate that FLAG-tagged Psb28-2 is present in both the monomeric PSII core complex and a PSII core complex lacking the inner antenna CP43 (RC47), whereas Psb28-1 preferentially binds to RC47. When cells are exposed to increased irradiance, both tagged Psb28 proteins additionally associate with oligomeric forms of PSII and with PSII-PSI supercomplexes composed of trimeric photosystem I (PSI) and two PSII monomers as deduced from electron microscopy. The presence of the Psb27 accessory protein in these complexes suggests the involvement of PSI in PSII biogenesis, possibly by photoprotecting PSII through energy spillover. Under standard culture conditions, the distribution of PSII complexes is similar in the wild type and in each of the single *psb28* null mutants except for loss of RC47 in the absence of Psb28-1. In comparison with the wild type, growth of mutants lacking Psb28-1 and Psb27, but not Psb28-2, was retarded under high-light conditions and, especially, intermittent high-light/dark conditions, emphasizing the physiological importance of PSII assembly factors for light acclimation.

Key words: Psb28 proteins, photosystem I and II, *Synechocystis*

Bečková M., Gardian Z., Yu J., Konik P., Nixon P.J., and Komenda J. (2017). Association of Psb28 and Psb27 Proteins with PSII-PSI Supercomplexes upon Exposure of *Synechocystis* sp. PCC 6803 to High Light. *Mol. Plant.* **10**, 62–72.

INTRODUCTION

The photosystem II (PSII) complex is the light-driven water-plastoquinone oxidoreductase of oxygenic photosynthesis, responsible for splitting water into molecular oxygen and releasing protons and electrons for the generation of the ATP and NADPH needed for the fixation of carbon dioxide in cyanobacteria, algae, and plants. The most active form of PSII is a dimer whose structure from thermophilic cyanobacteria is now known to a resolution of 1.9 Å (Umena et al., 2011). The PSII monomer features 17 transmembrane protein subunits, three peripheral proteins and about 80 cofactors (Guskov et al., 2009). The transmembrane reaction center (RCII) subunits D1 and D2 are essential for the binding of cofactors involved in primary charge separation and subsequent electron transfer (Diner et al., 2001).

The chlorophyll-containing CP47 and CP43 inner antenna complexes that deliver energy from the outer antennae to the reaction center are located on either side of the D1-D2 heterodimer. CP43 also has a role with D1 in binding the Mn₄CaO₅ cluster involved in water splitting (Ferreira et al., 2004).

Assembly of PSII is thought to be a stepwise process (Komenda et al., 2004) proceeding through several intermediate complexes. Initially, the large pigment proteins form pre-complexes (or modules) with small transmembrane polypeptides, pigments, and possibly other cofactors (Komenda et al., 2012b). First the D1

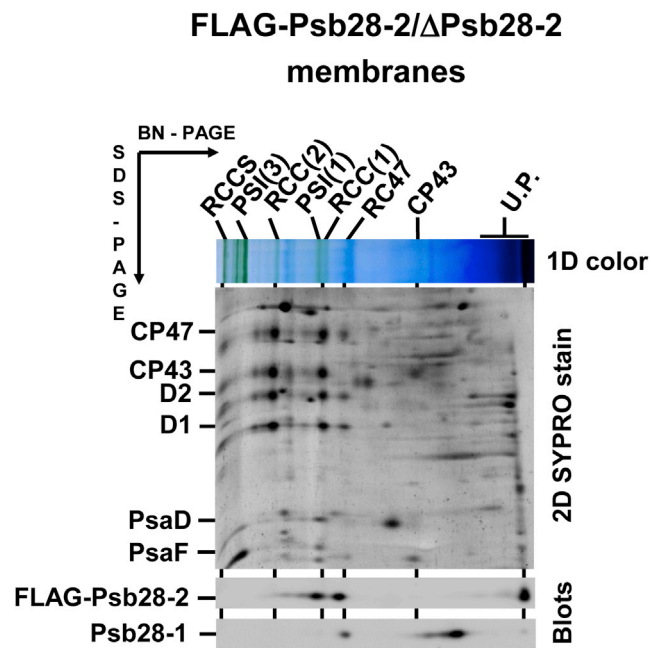


Figure 1. Two-Dimensional Protein Analysis of a *Synechocystis* 6803 Strain FLAG-Psb28-2/ Δ Psb28-2 Expressing the FLAG-Psb28-2 Protein Instead of Psb28-2.

Solubilized membranes isolated from the strain corresponding to 4 μ g of Chla were analyzed by blue-native PAGE in the first dimension (1D color) and by SDS-PAGE in the second dimension. The gel was stained with SYPRO orange (2D SYPRO stain); proteins were blotted onto PVDF membrane and subsequently probed with specific antibodies (Blots). The designation of complexes: RCCS, supercomplex of PSI trimer and PSII dimer; PSI(3) and PSI(1), trimeric and monomeric photosystem I; RCC(2) and RCC(1), dimeric and monomeric PSII core complexes; RC47, the monomeric PSII core complex lacking CP43; U.P., unassembled proteins.

and D2 modules form a reaction center intermediate complex (RCII) to which the CP47 module is attached to form a core complex lacking CP43 (termed RC47). Subsequent attachment of the CP43 module leads to the formation of a PSII monomeric core complex (RCC(1)) with assembly completed by dimerization to form RCC(2) (reviewed in Nixon et al., 2010). Light-driven assembly of the Mn_4CaO_5 cluster and attachment of the luminal extrinsic subunits is thought to occur after formation of RCC(1) (Nixon et al., 2010). Correct and efficient assembly of PSII is controlled by a number of auxiliary protein factors that are absent from the final functional PSII complex. Some of these, such as the Psb28 proteins (Pfam: PF03912), are highly conserved and are found both in cyanobacteria and chloroplasts.

The genome of the cyanobacterium *Synechocystis* sp. PCC 6803 (hereafter *Synechocystis* 6803) codes for two Psb28 homologs: Psb28-1 (encoded by gene *sll1398*) and Psb28-2 (encoded by gene *slr1739*) (Boehm et al., 2012). Psb28-1 (also named Psb13 and Ycf79) was first identified as a component of a His-tagged PSII preparation isolated from *Synechocystis* 6803 (Kashino et al., 2002) and, subsequently, shown to be a hydrophilic protein peripherally attached to the membrane (Dobáková et al., 2009). The absence of transmembrane structural motifs was later confirmed by the determination of the solution structure of His-tagged Psb28-1 by NMR (PDB: 2KVO; Yang

et al., 2011). Psb28-1 in *Synechocystis* 6803 most probably exists as a dimer (Bialek et al., 2013) and has been detected in the RC47 complex (Dobáková et al., 2009; Boehm et al., 2012; Sakata et al., 2013) in the vicinity of the PsbH subunit (Dobáková et al., 2009).

The phenotype of *psb28-1* null mutants of *Synechocystis* 6803 is controversial. The knockout mutant constructed by Dobáková et al. (2009) exhibited slower autotrophic growth, accelerated turnover of the D1 subunit, decreased synthesis of the CP47 inner antenna, and a lower cellular level of chlorophyll (Chl) in comparison with wild type (WT). In contrast, the phenotype of the null mutant described by Sakata et al. (2013) was much milder, showing just growth retardation under increased temperature, especially when combined with inactivation of the *dgdA* gene causing a defect in the biosynthesis of digalactosyldiacylglycerol.

The genomes of *Synechocystis* 6803 and some other cyanobacteria contain another *psb28* gene designated *psb28-2*. A knockout mutant of *Synechocystis* 6803 lacking Psb28-2 behaves like WT, and deletion of the *psb28-2* gene in the Psb28-1-less strain does not show an additional effect, indicating that Psb28-2 is not able to substitute for Psb28-1 (Sakata et al., 2013). The structure of Psb28-2 is thought to be similar to that of Psb28-1 (Mabbitt et al., 2014) except that it likely exists as a monomer (Bialek et al., 2013), due to the lack of several amino acid residues putatively involved in dimerization of Psb28 (Mabbitt et al., 2014). Psb28-2 like Psb28-1 has been detected in RC47 complexes (Boehm et al., 2012).

The physiological importance of Psb28 proteins in PSII assembly and function in *Synechocystis* 6803 remains unknown. Here we show that, under increased irradiance, both proteins together with Psb27, a luminal accessory protein associated with non-oxygen-evolving PSII core complexes (Nowaczyk et al., 2006), become components of PSII-PSI supercomplexes, the formation of which may be an important step in PSII biogenesis especially under high irradiance. Consistent with this, we show that growth of both the *Psb27* and *Psb28-1* mutants is affected under conditions of continuous and especially intermittent high light.

RESULTS

Differences in the Association of Psb28 Proteins with PSII

Previous work has shown that both Psb28-1 and Psb28-2 are able to bind to the RC47 complex (Dobáková et al., 2009; Boehm et al., 2012; Bialek et al., 2013). However, the weak Psb28-2 signal detected by immunoblotting in this earlier work prevented a complete analysis of the binding of Psb28-2 to other types of PSII complexes. To address this problem, we used commercial FLAG-tag specific antibodies to detect expression of a Psb28-2 derivative containing a 3xFLAG tag fused to the N terminus (FLAG-Psb28-2) (Boehm et al., 2012). Two-dimensional (2D) gel electrophoresis of solubilized thylakoids isolated from this strain confirmed the presence of the protein not only in RC47 but also at similar levels in the monomeric PSII core complex (RCC(1)) (Figure 1). Additional probing of the same blot with an antibody against Psb28-1 detected Psb28-1 just in RC47, in agreement with earlier work (Dobáková et al., 2009). The

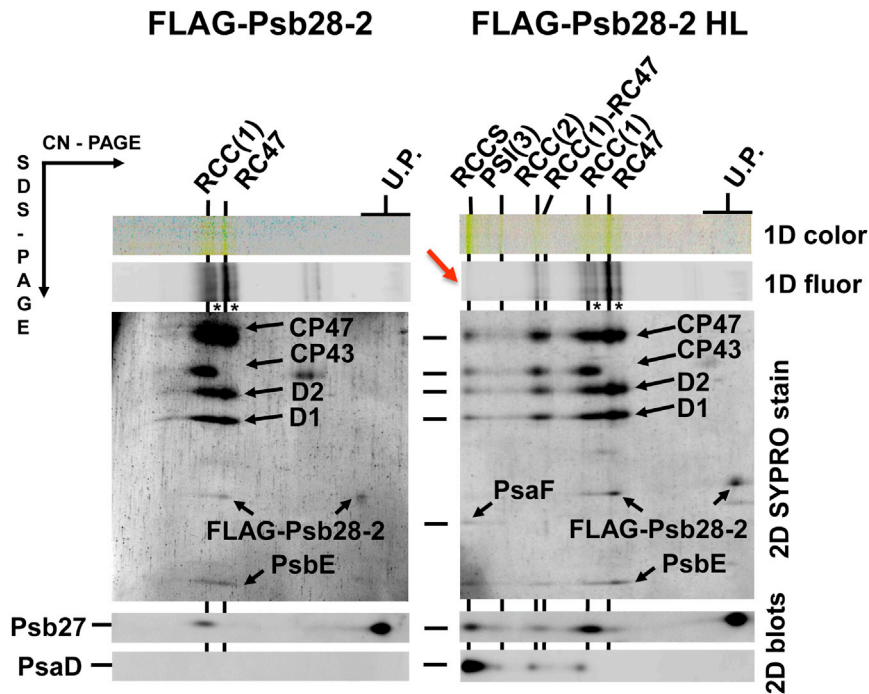


Figure 2. Two-Dimensional Protein Analysis of N-Terminally FLAG-tagged Psb28-2 Preparation (FLAG-Psb28-2) Isolated by Affinity Chromatography from Cells of FLAG-Psb28-2/ Δ Psb28-2 Strain Grown Under Low (Left) or High (HL, Right) Irradiance.

Preparations were analyzed by CN PAGE in the first dimension, and the native gel was photographed (1D color) and scanned with an LAS-4000 camera for Chl fluorescence (1D fluor); after SDS-PAGE in the second dimension, the gel was stained with SYPRO orange (2D SYPRO stain), electroblotted to PVDF membrane, and probed with the antibody specific for Psb27 and PsaD (2D blots). The designation of complexes as in Figure 1, RCC(1)-RC47 is a PSII dimeric core complex lacking one of the CP43 inner antenna. The red arrow points to the fluorescence quenching in RCCS. Asterisks indicate PSII complexes lacking FLAG-Psb28-2.

apparent masses of the RC47 complexes containing Psb28-1 and FLAG-Psb28-2 in RC47 were slightly different, suggesting that the two Psb28 proteins might not bind to the same complex. The position of unassembled Psb28-1 in the native gel was also in agreement with its postulated dimeric structure, whereas unassembled FLAG-Psb28-2 migrated as a monomer.

FLAG-Psb28-2-containing complexes immunopurified under mild solubilization conditions were also examined by 2D gel electrophoresis. In the first dimension, we used clear-native (CN) PAGE, which enables sensitive identification of PSII complexes directly in the gel due to the emission of Chl fluorescence. This analysis confirmed the association of FLAG-Psb28-2 with RC47 but, unlike a previous study (Boehm et al., 2012) (see also Supplemental Figure 1), we observed a monomeric PSII core complex RCC(1) in the pull-down experiment (Figure 2, left panel), possibly because the use of a milder MES buffer containing Mg^{2+} and Ca^{2+} ions stabilized binding of CP43 within the isolated RCC(1) complex during purification. Immunoblotting showed that RCC(1) complexes isolated using FLAG-Psb28-2 contained another PSII assembly factor, Psb27 (Figure 2). Both the RC47 and RCC(1) complexes were present in two versions: a larger one containing FLAG-Psb28-2 and a smaller one lacking FLAG-Psb28-2 as judged from the relative migration of the FLAG-tagged protein band (Figure 2, complexes with asterisks). This suggests that a sub-population of FLAG-tagged Psb28-2 is released from PSII complexes during native PAGE and migrates in the region of unassembled proteins. This is even better documented in Supplemental Figure 1 when the 2D gel analysis was performed using FLAG-tagged Psb28-2 isolated by the previously described method (Boehm et al., 2012).

Although the amount of SYPRO-stained FLAG-Psb28-2 in Figure 2 seemed to be sub-stoichiometric in comparison with the pulled down larger PSII proteins, comparison of the staining

obtained with SYPRO orange, used in this study due to its compatibility with immunoblotting, and with Coomassie blue (CBB)

(Supplemental Figure 1) showed that the reason is the lower stainability of the tagged Psb28-2 and other smaller proteins (e.g., PsbE) by SYPRO stain. Indeed, comparison of the approximate intensity ratio of the FLAG-Psb28-2 and CP47 in the SYPRO-stained and CBB-stained gels showed much higher value with CBB staining (Supplemental Figure 1).

To exclude the effect of the position of the FLAG tag on the binding specificity of the Psb28 proteins, we analyzed membranes of two other strains expressing either N-terminally tagged Psb28-1 or C-terminally tagged Psb28-2 (FLAG-Psb28-1 and Psb28-2-FLAG, respectively) from their native promoters (Supplemental Figure 2). Membrane protein analysis confirmed that the position of the tag did not affect the binding specificity of each of the Psb28 proteins to PSII since FLAG-Psb28-1 was found in RC47 and Psb28-2-FLAG in both RC47 and RCC(1) (Supplemental Figure 2). In addition, RC47 and RCC(1) were both pulled down by Psb28-2-FLAG (Supplemental Figure 3).

Both FLAG-Tagged Psb28 Proteins Associate with Large PSII-PSI Supercomplexes under Increased Irradiance

We found that exposure of cells to increased irradiance led to an altered composition of the resulting pull-down preparations. FLAG-Psb28-2 isolated from more illuminated cultures contained a higher proportion of dimeric PSII core complexes and, in addition, a non-fluorescent large Chl-protein complex visible at the edge of the CN gel (Figure 2, right panel). The 2D gel showed that the latter complex contained all four large PSII Chl-binding proteins, but its pigmentation was clearly higher than that of PSII core complexes. The absorption spectrum of the band showing a maximum at about 677 nm and a main 77 K fluorescence band peaking at 722 nm pointed to the presence of the photosystem I (PSI) complex (Figure 3, right panel). This was

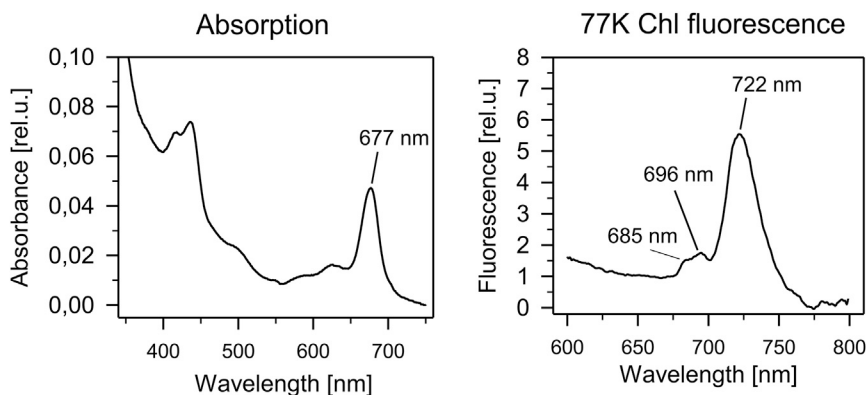


Figure 3. The Room Temperature Absorption (Left) and 77K Chl Fluorescence (Right) Spectra of the RCCS Band Cut from the CN Gel Shown in Figure 2 (Right).

The absorption spectrum was measured using a Shimadzu UV-3000 spectrometer; the fluorescence spectrum was measured using an Aminco Bowman Series 2 luminescence spectrometer.

further confirmed by mass spectrometry analysis, which showed the presence of the PsaA, PsaF, and PsaL subunits of PSI (Table 1). The presence of PSI in the complex was also confirmed by immunodetection of the PsaD protein; the weaker signals detected in smaller complexes most probably reflect the presence of PSI trimeric, dimeric, and monomeric complexes (Figure 2 and Supplemental Figure 2D blots). Therefore, we ascribe the large complex to a supercomplex of PSII and PSI (RCCS, Figure 2, right panel). In agreement with previously published data, the supercomplex also contained Psb27 (Komenda et al., 2012a), a luminal accessory protein associated with non-oxygen-evolving PSII core complexes (Nowaczyk et al., 2006), which suggests a role for the supercomplex in PSII assembly/repair. A similar pattern of PSII complexes was also obtained when we affinity purified C-terminally tagged Psb28-2 (Psb28-2-FLAG) from cells grown under standard and high irradiance (Supplemental Figure 3). The complexes again contained Psb27.

We further tested whether FLAG-tagged Psb28-1 also co-isolated with RCCS under increased irradiance. Psb28-1-FLAG co-purified with RC47, a very small amount of RCC(1) and RCC(1)-RC47 complex, when isolation was performed from cells grown under standard conditions (Figure 4, left panel). Here again the seemingly low level of the pulled down Psb28-1-FLAG was related to the weaker staining of the protein by SYPRO orange (Supplemental Figure 4). When isolated from cells exposed to high irradiance, the preparation additionally contained a significant amount of the PSII-PSI supercomplex (Figure 4, right panel). The presence of PSI was again confirmed by identification of both PsaD in the complex by immunoblotting (Figure 4 and 2D blots) and PsaE in the pull-down by mass spectrometry (Supplemental Table 1). We never identified Psb28-2 in Psb28-1-FLAG pull-down, confirming their independent binding (not shown).

To further characterize the PSII-PSI supercomplex, we subjected the Psb28-1-FLAG preparation to single-particle analysis. Due to the low amount of supercomplexes in the preparation (Figure 5A), the resolution of the obtained images was rather limited; nevertheless it was sufficient for the unequivocal identification of PSI trimers in the particles. The shape and size of the additional structures attached to the PSI trimer corresponded well to two monomeric PSII complexes (Figure 5B). Results from single-particle analysis also supported the presence of RCC(1)-RC47 complexes (Figure 5C), which

were detected by 2D gel electrophoresis on the basis of a relative decrease in intensity of the CP43 band in the complex compared with RCC(1) complexes (Figure 4).

The PSII-PSI supercomplexes were present in WT cells even under standard light conditions, and their quantity only slightly increased after exposure of the cells to high light (Supplemental Figure 5). These data indicate that these complexes are constitutively present in cells, but after high-light treatment there is an increase in the amount of a specific fraction that binds the Psb28 and Psb27 proteins.

We also tested unspecific binding of RCCS and other PSII complexes to FLAG-affinity resin using solubilized membranes from the control WT strain subjected to high irradiance. No apparent Chl-containing complexes present in the eluate excluded an artificial binding of RCCS to the affinity resin (Supplemental Figure 5).

Differences in the Profile of PSII Complexes in *psb28* Null Mutants

Previous results have suggested that the strain lacking Psb28-1 shows impaired synthesis of CP47 and PSI and accumulates lower levels of Chl in the cell (Dobáková et al., 2009). However, this phenotype was not observed in a second independently constructed *psb28-1* mutant (Sakata et al., 2013). Since this disagreement could be caused by differences in the genetic backgrounds of the two WT strains used to make the mutants, we constructed two new Psb28-1- and Psb28-2-less mutants using a different WT strain. In our original study (Dobáková et al., 2009), we used a WT strain very similar to the glucose-tolerant GT-O2 strain (Morris et al., 2014), which was subsequently shown to exhibit partial Chl depletion upon autotrophic growth conditions (GT-W; Tichý et al., 2016). The new set of mutants was instead constructed in the GT-P strain similar to the GT-Kazusa strain (Supplemental Figure 6), which contains a similar content of Chl as the standard motile PCC 6803 strain (Tichý et al., 2016). The resulting *psb28* mutants were found to have a similar cellular Chl content as the control and contained very similar levels of PSI and both monomeric and dimeric PSII core complexes as revealed by CN gel electrophoresis (Figure 6) in agreement with Sakata et al. (2013). This result indicates that the decreased level of Chl in the *psb28-1*-less strain seen by Dobáková et al. (2009) was most probably related to the Chl-deficient phenotype of the WT strain originally used for mutant construction.

Nevertheless, when we performed radioactive labeling of proteins in the new strains, the *psb28-1*-less mutant still showed lower labeling of CP47 and PSI in comparison with the other

Protein, UniProtKB no.	Size (Da), length (no. of amino acids)	Coverage (%)	Detected/theoretical no. of peptides	PLGS score
CP47, P05429	55 903, 507	5	1/27	208
D1, P14660	39 695, 360	3	1/14	130
PsaA, P29254	82 950, 751	5	3/34	338
PsaF, P29256	18 249, 165	19	2/11	95
PsaL, P37277	16 624, 157	25	2/6	160

Table 1. List of Proteins Identified by Mass Spectrometry in the CN-PAGE-Separated PSII-PSI Supercomplex RCCS of the Psb28-2-FLAG Pull-Down (Figure 2) Isolated from High-Light-Treated Cells of the *Synechocystis* Strain Expressing Psb28-2-FLAG.

The PLGS score is a statistical measure of peptide assignment accuracy; it is calculated with Protein Lynx Global Server (PLGS 2.2.3) software (Waters).

two strains (Supplemental Figure 7). Another common feature of the new Δ Psb28-1 strain shared with the one constructed by Dobáková et al. (2009) was the lack of detectable RC47 complex and a lower level of free unassembled CP47, while in the strain lacking Psb28-2, the RC47 complex was clearly visible and was even more abundant than in WT (Figure 6, right panel and quantification table). All three strains show the presence of PSI-PSII supercomplexes under both standard and high-light conditions indicating that the accumulation of PSII supercomplexes is not dependent on the presence of Psb28 proteins.

Loss of Psb28-1 but Not Psb28-2 Impairs Growth in Continuous High Light and Especially Intermittent Light

Under standard illumination conditions, growth of the *psb28-1* and *psb28-2* null mutants on agar plates was indistinguishable to WT (Figure 7, left panels). Under high irradiance, the strain lacking Psb28-1 grew slightly slower than the WT and Psb28-2-less strains but its sensitivity to high light was exacerbated when we used intermittent (5 min dark and 5 min 400 $\mu\text{mol photons m}^{-2} \text{s}^{-1}$) instead of continuous (400 $\mu\text{mol photons m}^{-2} \text{s}^{-1}$) high light (Figure 7, upper right panel). When the *psb28-2* gene was additionally inactivated in the Psb28-1 mutant, the growth of the resulting double mutant was identical to that of the *psb28-1* mutant under all tested conditions (not shown). A *psb27* null mutant also grew more slowly under intermittent light in comparison with WT (Figure 7, lower right panel). Finally, we constructed the Psb27/Psb28-1 double mutant, which showed the slowest growth of all the tested strains in high continuous light and did not grow at all in intermittent light.

As the Psb28-1-less strain showed a light-sensitive phenotype, we checked whether it is a light-inducible stress protein like members of the family of high-light-inducible proteins (Hlips, He et al., 2001). While the level of Psb28-1 remained the same after 2 h exposure of WT cells to 500 $\mu\text{mol photons m}^{-2} \text{s}^{-1}$, the content of HliA/B in these cells sharply increased, meaning that pool of Psb28-1 in the cell is stable and the protein is not high-light inducible.

DISCUSSION

Many cyanobacteria, like *Synechocystis* 6803, encode two different Psb28 proteins. Here we confirm that under standard cultivation conditions both Psb28-1 and Psb28-2 associate with the RC47 complex. One difference between the two forms of Psb28 is that Psb28-2 is found at higher levels in the mono-

meric RCC(1) complex (Figures 1, 2, and 4). When the Psb28 proteins were purified from cells exposed to increased irradiance, oligomeric PSII complexes, small amounts of PSI, and especially PSII-PSI supercomplexes now appeared in the affinity-purified preparations. Interestingly, the Psb27 assembly factor was also present in these complexes in accordance with previous results indicating a close relationship between Psb27 and Psb28 proteins (Kashino et al., 2002; Liu et al., 2011a, 2011b; Nowaczyk et al., 2012). Association of Psb27 with large PSI-PSII complexes has also been demonstrated in previous studies (Liu et al., 2011b; Komenda et al., 2012a). Given that Psb27 is associated with PSII complexes lacking a functional oxygen-evolving complex (Nowaczyk et al., 2006), the complexes containing both Psb27 and Psb28 are therefore likely to be involved in de novo assembly and/or repair of PSII.

Single-particle analysis of preparations isolated using FLAG-tagged Psb28 proteins from high-light exposed cells showed the presence of large particles containing PSI trimer together with two additional densities corresponding in size and shape to two PSII monomers; however, the organization of the two monomers is clearly different from their arrangement in the known dimeric crystal structures, which would suggest binding to trimeric PSI as monomers rather than a dimer (Figure 5). The close association of PSI trimeric complexes with PSII complexes containing the Psb28 and Psb27 assembly factors supports our previous hypothesis that PSI might play a protective role during PSII biogenesis (Komenda et al., 2012a). Indeed this association between PSII and PSI in the supercomplexes resulted in the loss of Chl fluorescence of otherwise highly fluorescent PSII complexes, indicating efficient energy spillover to PSI (Figures 2 and 4). Thus, the formation of PSI-PSII supercomplexes might reflect a light-induced response of the PSII assembly machinery to protect PSII assembly complexes via efficient PSI-mediated quenching of harmful excitation energy absorbed by these intermediates. Moreover, as we have recently identified trimeric PSI as the main sink for newly synthesized Chl (Kopečná et al., 2012), association of PSII assembly complexes with PSI trimeric complexes may also allow production of PSII assembly modules using Chl released from trimeric PSI.

The crystal structure of Psb28 from *Thermosynechococcus elongatus* suggests that the proximity of the C termini of the two monomers in the dimer does not allow tagging of the molecule without destabilization of the dimer, and this was supported by

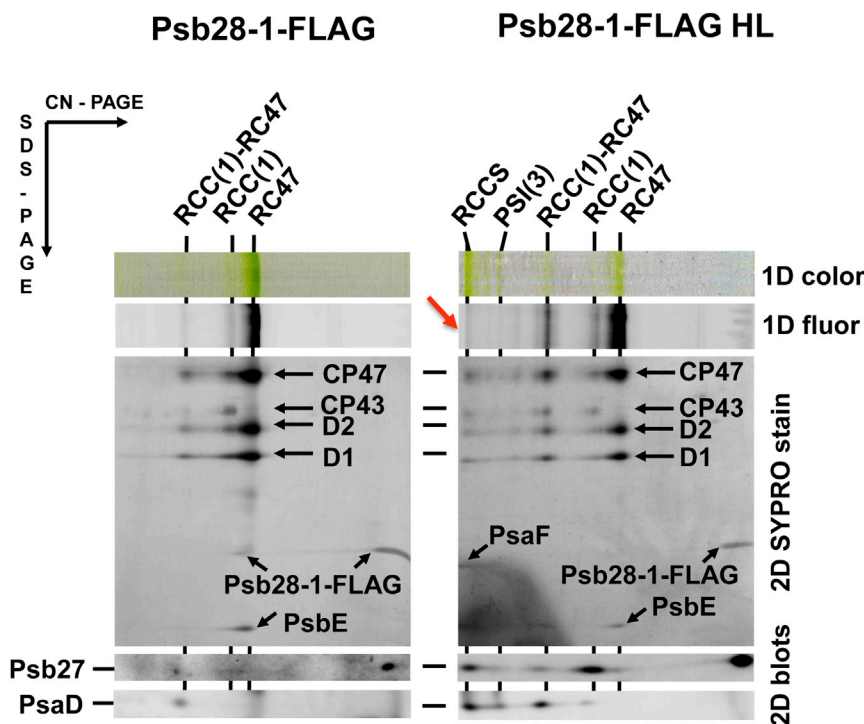


Figure 4. Two-Dimensional Protein Analysis of FLAG-tagged Psb28-1 Preparation Isolated by Affinity Chromatography from Cells of Psb28-1-FLAG/ Δ Psb28-1 Strain Grown Under Low (Left) or high (HL, Right) Irradiance.

Preparations were analyzed by CN PAGE in the first dimension, and the native gel was photographed (1D color) and scanned by an LAS-4000 camera for Chl fluorescence (1D fluor); after SDS-PAGE in the second dimension, the gel was stained with SYPRO orange (2D SYPRO stain), electroblotted to PVDF membrane, and probed with the specific antibodies against Psb27 and PsaD (2D blots). The designation of complexes as in Figure 1, RCC(1)-RC47 is a PSII dimeric core complex lacking one of the CP43 inner antenna. The red arrow points to the fluorescence quenching in RCCS.

analysis of the strain expressing Psb28-1 with an FLAG tag on the C terminus. Nevertheless, the FLAG-tagged protein was still able to bind to RC47 in cells (Supplemental Figure 2, left) and PSII copurified with the isolated tagged protein, suggesting that the dimeric structure of the Psb28-1 protein is not needed for binding to PSII (Figure 4).

Binding of Psb28 proteins to PSII is dependent on the presence of PsbH (Dobáková et al., 2009; Bialek et al., 2013); this fact, together with the inhibitory effect of deleting *psb28-1* on synthesis of CP47, led to speculation that Psb28-1 is bound to CP47. However, taking into account the oligomeric structure of native Psb28-1 together with the presence of a long N-terminal helix of PsbH stretching over CP47, it is also possible that Psb28 binds more in the center of PSII than previously envisaged and so prevents binding of CP43 to RC47 thereby allowing accumulation of RC47 in the membrane.

PsbH is also essential for the binding to PSII of HliB (also termed ScpD), a member of the family of high-light-inducible proteins (Hlips) (He et al., 2001) or small chlorophyll-a/b-binding-like proteins (Scps) (Funk and Vermaas, 1999). We show that expression of Hlips is quickly induced upon increase of irradiance, while the Psb28-1 protein is present constitutively in cells and its content does not respond to high light (Figure 8). Although we cannot exclude that all Psb28-1 proteins weakly interact with PSII in the membrane and this interaction is disrupted during native PAGE, there is nevertheless a fraction of Psb28-1 that binds to RC47 more stably and which is identified in the native gels as the component of the complex (Figure 1; Dobáková et al., 2009). Thus, it seems that the Psb28-1 protein is available for binding to PSII before the production of Hlips and that its prompt binding may be important for Psb28-1 function during high/intermittent light stress.

2013) suggest that Psb28-2 is not a redundant Psb28-1 copy with the same function. Instead, we speculate that Psb28-2 may act as an antagonist that prevents formation of RC47 by excluding Psb28-1 from its binding site. That the two Psb28 proteins might play different roles is in line with the upregulation of the *psb28-1* transcript level but downregulation of *psb28-2* in a *Synechocystis* 6803 mutant lacking the PsbO protein (Schriek et al., 2008), which is highly sensitive to photoinhibition and exhibits very fast D1 turnover (Komenda and Barber, 1995). Similarly, the expression profiles of the *psb28-1* and *psb28-2* genes were found to be quite different under a variety of environmental conditions in a very recent transcriptomic study (Hernández-Prieto et al., 2016), again supporting a distinct functional role for each protein.

In the absence of Psb28-1, the RC47 complex is undetectable in cells grown under standard conditions, while in WT cells this complex is detectable. This difference has previously been related to an effect on CP47 synthesis as the *psb28-1*-null mutant contains an increased level of RCII, the assembly complex that immediately precedes RC47 in the PSII assembly pathway (Dobáková et al., 2009). For the newly constructed *psb28-1* mutant described here, there was also reduced synthesis of CP47 (autoradiogram in Supplemental Figure 7). Interestingly, unlike the *Synechocystis* 6803 CP43-less mutant, the CP47-less mutant shows a Chl-deficient phenotype reflecting reduced PSI accumulation (Supplemental Figure 8), and the decreased synthesis of PSI detected in the *psb28*-null mutant could similarly be related to the lower synthesis of CP47 (autoradiogram in Supplemental Figure 7). A specific effect on the synthesis of PSI and CP47 has also been seen in the Δ por (Kopečná et al., 2013) and Δ gun4 (Sobotka et al., 2008) mutants disrupted in the PChlide reduction and Mg-chelatase steps, respectively, and in the *ycf54* mutant affected

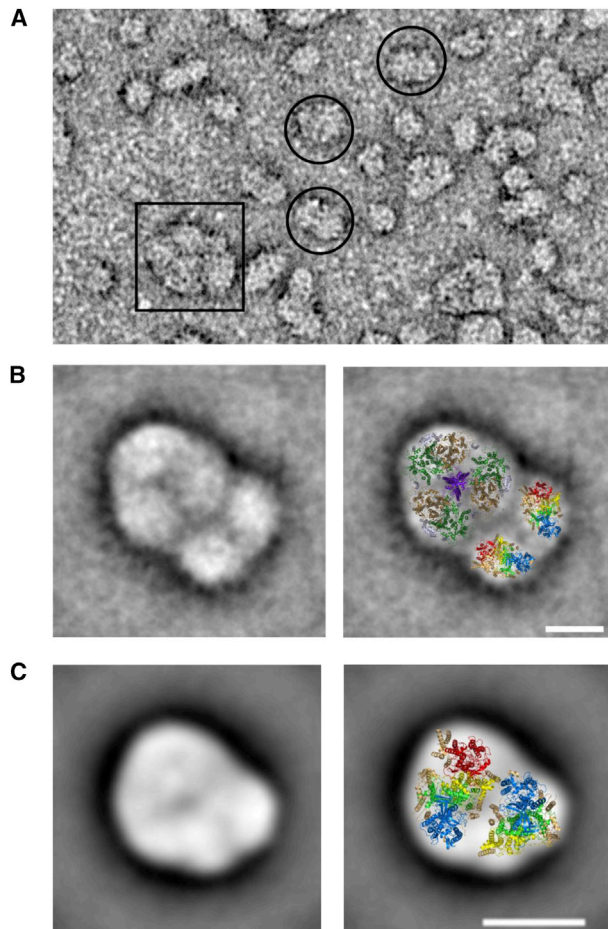


Figure 5. Electron Microscopic Analysis of Complexes Co-isolated with Psb28-1-FLAG from High-Light Exposed Culture.

(A) Electron micrographs of negatively stained complexes. The labeled RCCS and RCC(1)-RC47 particles are in square and circles, respectively. **(B)** The top view projection map of the RCCS supercomplex containing trimeric PSI complex and two PSII monomers. The negatively stained particle (left) was obtained by classification of 95 particles. Right: the projection was overlaid with a cyanobacterial X-ray models of the PSI trimer and two PSII core complexes. **(C)** The negatively stained particles of RCC(1)-RC47 (left) was obtained by classification of 5600 particles. The projection was overlaid with a cyanobacterial X-ray model of the PSII monomer and PSII monomer lacking CP43 and associated proteins (PsbK, PsbZ, and Psb30). Color designation of proteins: PsaA, brown; PsaB, dark green; PsaL, violet; other small PSI subunits, gray; D1, yellow; D2, light green; CP47, blue; CP43, red; small PSII subunits, ochre. The coordinates are taken from the PDB (<http://www.rcsb.org/pdb>): PSI code, PDB: 1JB0 (Jordan et al., 2001); PSII code, PDB: 2AXT (Loll et al., 2005). The scale bars represent 10 nm.

in the function of aerobic cyclase involved in the synthesis of the fifth Chl ring (Hollingshead et al., 2016). Given that newly synthesized Chl in *Synechocystis* 6803 is preferentially incorporated into the PSI trimer (Kopečná et al., 2012) and that this complex is particularly deficient in the CP47-less, Δpor and $\Delta gun4$ mutants, Psb28-1 could regulate this main pathway for Chl incorporation. A link between Psb28-1 and the synthesis of Chl-binding proteins is also suggested from analysis of gene transcription during the diurnal cycle of the

nitrogen-fixing cyanobacterium *Cyanothece* sp. ATCC 51142. Unlike transcripts for other PSII-associated genes, *psb28* transcripts preferentially accumulate during the dark period when Chl biosynthesis is activated and PSI proteins in particular are synthesized, probably in readiness for the start of the light period (Stöckel et al., 2011).

Previous studies on *psb28* mutants constructed in *Synechocystis* 6803 have led to conflicting results regarding the importance of Psb28-1 for accumulation and assembly of both photosystems. By constructing new deletion mutants in a WT strain of *Synechocystis* 6803 that is known not to be affected in chlorophyll biosynthesis, we have confirmed that Psb28-1 has very little impact on growth under standard continuous illumination ($40 \mu\text{mol photons m}^{-2} \text{s}^{-1}$). Importantly, we have been able to show here that Psb28-1 and Psb27 are needed for optimal growth especially under intermittent high-light/dark conditions (Figure 7). This phenotype has not been reported before for cyanobacteria. In the case of higher plants, Psb28 is already known to be required for normal growth and pigmentation of rice plants (Jung et al., 2008). The mechanism of Psb28-1 action remains unclear, but it apparently differs from that of Psb27, since the intermittent high-light/dark condition affected the growth of the Psb27/Psb28-1 double mutant more severely than each of the single mutants (Figure 7).

METHODS

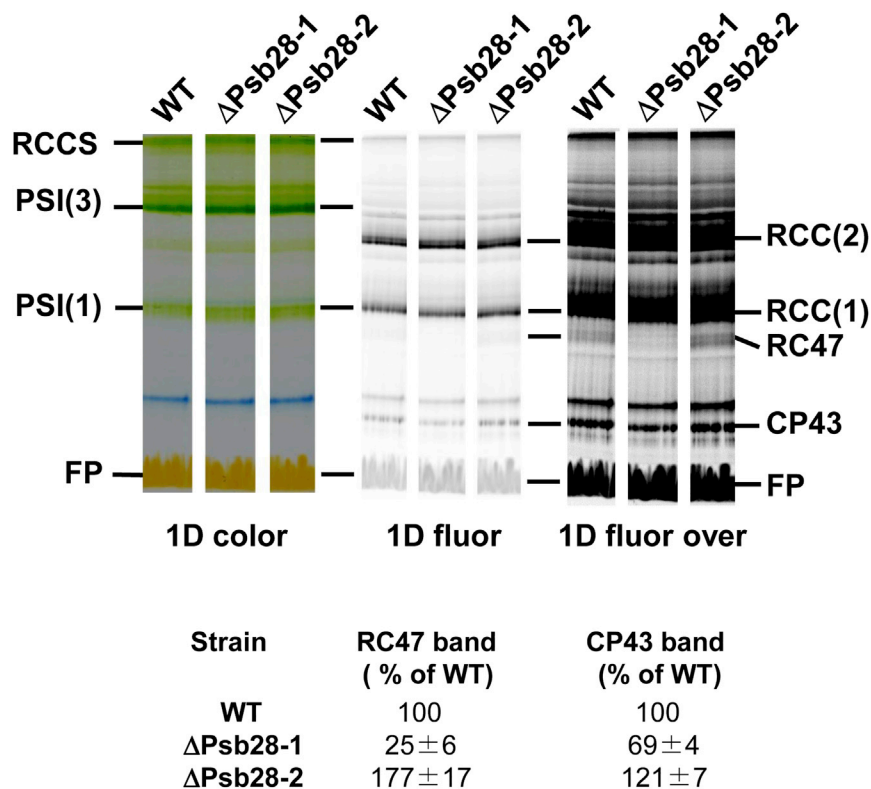
Construction of Mutant Strains

The non-motile, glucose-tolerant strain of *Synechocystis* sp. PCC 6803 GT-P (Tichý et al., 2016) was used in this study as a WT strain and as a background for the generated deletion mutant strains ($\Delta\text{Psb28-1}$, $\Delta\text{Psb28-2}$, $\Delta\text{Psb28-1}/\Delta\text{Psb28-2}$, and $\Delta\text{Psb27}/\Delta\text{Psb28-1}$) and FLAG-tagged mutants (Psb28-1-FLAG, FLAG-Psb28-1, Psb28-2-FLAG, and FLAG-Psb28-2).

Deletion Mutant Strains

The *psb28-1* knockout vector was constructed in two steps. First, the upstream region of *sl1398* was PCR amplified from WT genomic DNA of *Synechocystis* PCC 6803 with the primer set SII1398-1F and SII1398-2R, and the downstream region was amplified with SII1398-3F and SII1398-4R. The resulting PCR fragments were then mixed together to serve as the DNA template to perform overlap extension PCR with primer set SII1398-1F and SII1398-4R. The joint PCR fragment, which has the entire *sl1398* ORF replaced with an EcoRV restriction site, was cloned into pGEM-T Easy vector (Promega). The resulting plasmid, namely pGEM-SII1398, was then used as an intermediate vector for insertion of either kanamycin or chloramphenicol cassette via an EcoRV restriction site to create the final transformation vectors termed pSII1398Cam and pSII1398Kan (Supplemental Figure 6). The sequencing confirmed that the orientation of the resistance cassette was the same as the orientation of the gene of interest. The plasmid pSII1398Cam was used for transformation of the WT and ΔPsb27 strain to create deletion mutants $\Delta\text{Psb28-1}$ and $\Delta\text{Psb27}/\Delta\text{Psb28-1}$, respectively. The segregation was checked by PCR. Transformants were selected for Cam^R antibiotic resistance and PCR was used to show integration of the selectable marker and elimination of the WT gene copy.

The *psb27* and *psb28-2* knockout vector was constructed using an identical approach. The resulting plasmids pGEM-SIr1645 and pGEM-SIr1739 were then used as intermediate vectors for insertion of gentamicin, kanamycin, or chloramphenicol cassette via EcoRV restriction site to create the final transformation vectors termed pSir1645Gent, pSir1739Kan, and pSir1739Cam. The pSir1739Cam, which has a chloramphenicol



resistance cassette, was used for transformation of WT to create a deletion mutant ΔPsb28-2 and the pSlr1739Kan for transformation of the ΔPsb28-1 strain with Cam^R to create a double mutant ΔPsb28-1/ΔPsb28-2. The pSlr1645Gent was used for transformation of WT to create a deletion mutant ΔPsb27. Segregations were again checked by PCR. The transcription orientation of antibiotic cassettes was again along the genes of interest.

FLAG-Tagged Mutant Strains

The constructs Sll1398C/FLAG and Slr1739C/FLAG, designed to place the C-terminally FLAG-tagged *sll1398* and *slr1739* genes under the native promoters, consist of an upstream region, a gene with three repetitions of an eight amino acid FLAG sequence (3 × AspTyrLysAspAspAspLys; Sigma-Aldrich) on the C terminus, a zeocine cassette in reversed orientation, and downstream region of the corresponding gene (Supplemental Figure 9, right). The constructs were commercially synthesized and cloned to the pUC57 plasmid by EcoRV (Gene Synthesis Service, GenScript; Supplemental Figure 9, left). The obtained plasmids pUC57Sll1398C/FLAG and pUC57Slr1739C/FLAG were then used to transform the WT cells to yield strains expressing C-terminally FLAG-tagged Psb28-1 and Psb28-2. The complete segregation was checked by PCR (data not shown).

To create N-terminally FLAG-tagged Psb28-1, the pUC57Sll1398C/FLAG plasmid was used to generate pUC57Sll1398N/FLAG vector by replacing *sll1398*-FLAG with the FLAG-*sll1398* sequence using NdeI and AvrII restriction sites. The N-terminally FLAG-tagged Psb28-2 was placed under the *petJ* promoter in a ΔPsb28-2 background (Boehm et al., 2012).

Cultivation Conditions of Cyanobacterial Strains

The cells used in this study were grown in 100 mL of liquid BG11 medium using 250 mL flasks on an orbital shaker at 29°C under continuous light of 40 μmol photons m⁻² s⁻¹ (normal light). For (photo)heterotrophic growth conditions, the medium was supplemented with 5 mM glucose.

Figure 6. Pigment-Protein Analysis of Membranes Isolated from WT, ΔPsb28-1, and ΔPsb28-2 *Synechocystis* 6803 Strains by CN PAGE.

Strains were grown at irradiance of 40 μmol photons m⁻² s⁻¹. Each sample contained 4 μg of Chla corresponding to the same OD_{750 nm}. The native gel was photographed (1D color) and scanned with an LAS-4000 camera for Chl fluorescence before (1D fluor) and after enhancement of the signal (1D fluor over). Signals of RC47 and CP43 in 1D fluor were quantified with ImageQuant software and expressed as % of the WT band intensity. The values represent means of three independent measurements ± SD.

The cells used for protein purification were grown in 4 L of BG11 medium containing 1 mM glucose using 10 L flasks. The culture was air bubbled, stirred, and incubated at 29°C under continuous surface illumination of 120 μmol photons m⁻² s⁻¹ from a light source placed on one side of the flask (creating low-light conditions, due to the big volume of the culture). For high-light cultivation, the cells were grown in 400 mL of liquid BG11 medium using 1 L flasks containing 1 mM glucose and cultivated on an orbital shaker under gradually increasing surface illumination of 20–120 μmol photons m⁻² s⁻¹. WT cells were always grown under the same conditions as the mutant strains.

Growth Assay on Agar Plates

Cells of *Synechocystis* 6803 strains used for growth assay were cultivated autotrophically in 70 mL of liquid BG11 medium using 250 mL flasks on an orbital shaker at 29°C under continuous light of 40 μmol photons m⁻² s⁻¹ (normal light). After reaching the exponential phase, the cells were diluted to OD_{750 nm} 0.1, 0.05, and 0.025 and spotted on autotrophic BG11 agar plates containing 10 mM TES/NaOH, pH 8.2. One plate was always incubated at 40 μmol photons m⁻² s⁻¹ for 4 days, and identical plate was incubated under intermittent light conditions (5 min dark and 5 min 400 μmol photons m⁻² s⁻¹) or continuous high light (400 μmol photons m⁻² s⁻¹) for 4 days.

Radioactive Labeling

Radioactive pulse labeling of the cells was performed at 500 μmol photons m⁻² s⁻¹ and 30°C using a mixture of [³⁵S]Met and [³⁵S]Cys (Trans-label, MP Biochemicals) as described previously (Dobáková et al., 2009).

Protein Analysis

The Chla content of the samples was determined by extraction into methanol and absorption measurements at 666 and 720 nm (Wellburn, 1994).

Membranes were prepared by breaking the cells with zirconia/silica beads in A buffer (25 mM MES/NaOH [pH 6.5], 10 mM CaCl₂, 10 mM MgCl₂, and 20% glycerol). The broken cells were centrifuged at 20,000 *g* for 20 min and the pelleted thylakoid membranes were then resuspended in half volume of the supernatant, which represents the soluble fraction, in buffer A. The Chl concentration of 1% (w/v) *n*-dodecyl-β-D-maltoside solubilized membranes was measured by extraction into methanol and absorption measurements at 666 and 720 nm.

Thylakoid membranes corresponding to 4 μg of Chla were solubilized with 1% (w/v) *n*-dodecyl-β-D-maltoside and separated on a 4%–14% (w/v)

Molecular Plant

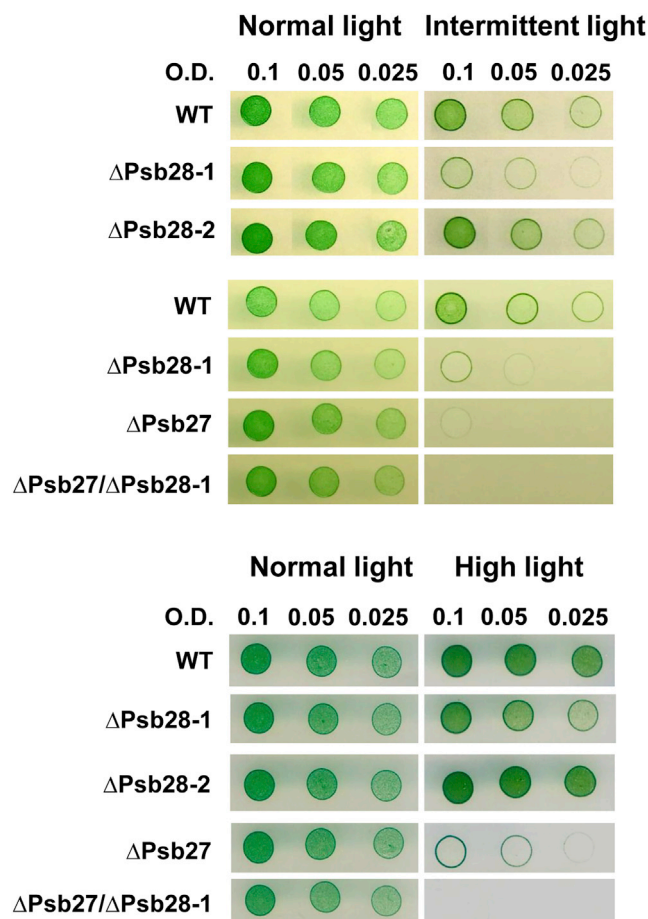


Figure 7. Growth Assay on Agar Plates of WT, Δ Psb28-1, Δ Psb28-2, Δ Psb27, and Δ Psb27/ Δ Psb28-1.

Each strain was cultivated autotrophically in liquid BG11 medium at $40 \mu\text{mol photons m}^{-2} \text{s}^{-1}$. After reaching the exponential phase, the cells were diluted to $\text{OD}_{750 \text{ nm}}$ 0.1, 0.05, and 0.025 and spotted on autotrophic agar plates. Identical plates were incubated for 4 days either at $40 \mu\text{mol photons m}^{-2} \text{s}^{-1}$ (left) or under intermittent light conditions (5 min dark and 5 min $400 \mu\text{mol photons m}^{-2} \text{s}^{-1}$, upper right) or at constant high light ($400 \mu\text{mol photons m}^{-2} \text{s}^{-1}$, lower right).

polyacrylamide CN PAGE linear gradient gel (Wittig et al., 2007) or a 4%–14% (w/v) polyacrylamide blue-native PAGE linear gradient gel (Komenda et al., 2012a). Chl fluorescence of separated PSII complexes was recorded using an LAS-4000 camera (Fujifilm, Japan). Gel stripes from the first dimension were incubated in 25 mM Tris/HCl buffer (pH 7.5) containing 1% DTT (w/v) and 1% SDS (v/v) at room temperature for 30 min and then separated on 12%–20% (w/v) polyacrylamide SDS-PAGE gel containing 7 M urea, the second dimension. The gels were stained either with CBB or, for immunoblotting, with fluorescence dye SYPRO orange (Sigma-Aldrich), blotted onto PVDF membrane, and subsequently used for immunodetection. Membranes were incubated with specific primary antibodies raised against Psb27 and PsaD (Komenda et al., 2012a), Psb28 (Dobáková et al., 2009), FLAG (Abgent), and HliA/B (Agrisera), and then with secondary antibody horseradish peroxidase conjugate (Sigma-Aldrich). After incubation with chemiluminescent substrate, Luminata Crescendo (Merck) blots were scanned with an LAS-4000 camera.

Isolation of FLAG-Tagged Proteins

For isolation of FLAG-tagged proteins, membranes were prepared by breaking the cells with zirconia/silica beads in buffer A (25 mM MES/

Function of Psb28 Proteins in *Synechocystis*

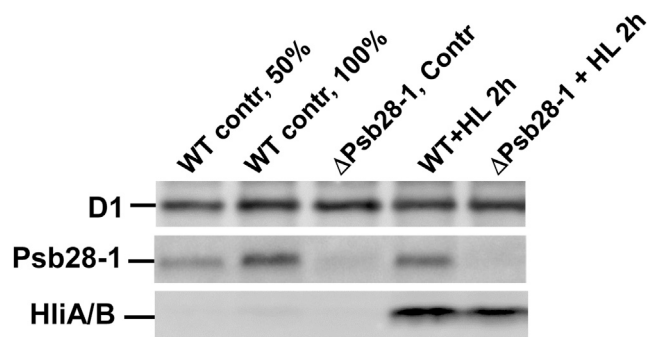


Figure 8. Protein Analysis of WT and Δ Psb28 Cells Grown under Standard (contr) and High ($500 \mu\text{mol photons m}^{-2} \text{s}^{-1}$) Irradiance for 2 h (HL 2h).

Membranes isolated from the cells corresponding to 4 μg of Chla (only lane designated WT contr, 50% contained 2 μg of Chla) were separated by SDS-PAGE, and proteins were blotted onto PVDF membrane and subsequently probed with antibody specific to the D1 protein (loading control), Psb28-1, and HliA/B.

NaOH [pH 6.5], 10 mM CaCl_2 , 10 mM MgCl_2 , and 25% glycerol) with protease inhibitor (SIGMAFAST Protease Inhibitor Cocktail Tablets, EDTA-Free, Sigma-Aldrich), separated from the soluble fraction by centrifugation at $60,000 g$ for 20 min; pelleted membranes were resuspended in buffer A and solubilized in 1.5% (w/v) *n*-dodecyl- β -D-maltoside. The supernatant was then loaded onto a column containing 300 μL of anti-FLAG M2 affinity gel (Sigma-Aldrich) pre-equilibrated with buffer A containing 0.04% *n*-dodecyl- β -D-maltoside (A-DDM buffer). To remove any loosely bound contaminants, the column was first washed with 5 mL of buffer A-DDM and then the FLAG-tagged protein was eluted by a 30 min incubation of resin in 200 μL of A-DDM buffer containing 20% glycerol and 150 μL of 3xFLAG peptide (Sigma-Aldrich). Resin was removed by centrifugation at $500 g$ for 5 min. The preparations obtained were separated by 2D gel electrophoresis with subsequent western blotting or Coomassie staining.

Spectroscopy Analysis

Chl fluorescence emission spectra at 77 K were measured using an Aminco Bowman Series 2 luminescence spectrometer (Spectronic Unicam) and fluorescence spectra were recorded in the range 600–800 nm.

Absorption spectra of whole cells and FLAG preparations were recorded in the range 350–750 nm using a Shimadzu UV-3000 spectrophotometer.

Transmission Electron Microscopy

Freshly prepared complexes were used for electron microscopy. The specimens were placed on glow-discharged carbon-coated copper grids and negatively stained with 2% uranyl acetate, visualized by a JEOL JEM-2100F transmission electron microscope (JEOL Japan, using 200 kV at $20,000\times$ magnification) and processed by image analysis. Transmission electron microscopy images were recorded with a bottom-mount Gatan CCD Orius SC1000 camera, corresponding to a pixel size of 3.4 Å. Image analyses were carried out using the Spider and Web software package (Frank et al., 1996). The selected projections were rotationally and translationally aligned, and treated by multivariate statistical analysis in combination with a classification procedure (Van Heel and Frank, 1981; Harauz et al., 1988). Classes from each of the subsets were used for refinement of alignments and subsequent classifications. For the final sum, the best of the class members were summed using a cross-correlation coefficient of the alignment procedure as a quality parameter. The projection was overlaid with cyanobacterial X-ray models of PSI (PDB: 1JB0, Jordan et al., 2001) and monomer of PSII core complexes (PDB: 2AXT, Loll et al., 2005).

Protein Identification by Mass Spectrometry

The MS analyses of protein bands excised from the gel or the liquid pull-down preparations of the tagged proteins were done on a NanoAcquity UPLC (Waters) coupled online to an ESI Q-ToF Premier mass spectrometer (Waters) as described in Janoušek et al. (2013).

SUPPLEMENTAL INFORMATION

Supplemental Information is available at *Molecular Plant Online*.

FUNDING

We gratefully acknowledge support from the Grant Agency of the Czech Republic (project P501/12/G055), the Czech Academy of Sciences (RVO 60077344 and RVO61388971), the Czech Ministry of Education (projects LO1416 and CZ 1.05/2.1.00/19.0392) and BBSRC (projects BB/L003260/1 and BB/I00937X/1).

AUTHOR CONTRIBUTIONS

M.B. constructed the strains expressing FLAG-tagged Psb28 proteins, performed most of the biochemical experiments, and participated in writing; Z.G. carried out the electron microscopy study; J.Y. constructed the Psb28 deletion mutants; P.K. performed the mass spectrometric analyses; P.J.N. planned the research, evaluated data, and drafted the manuscript; J.K. planned the research, participated in the experimental design and in experiments, evaluated data, and drafted the manuscript.

ACKNOWLEDGMENTS

We thank Eva Prachová and Jiří Šetlík for excellent technical assistance. No conflict of interest declared.

Received: March 20, 2016

Revised: June 29, 2016

Accepted: August 4, 2016

Published: August 12, 2016

REFERENCES

- Bialek, W., Wen, S., Michoux, F., Bečková, M., Komenda, J., Murray, J.W., and Nixon, P.J. (2013). Crystal structure of the Psb28 accessory factor of *Thermosynechococcus elongatus* photosystem II at 2.3 Å. *Photosynth. Res.* **117**:375–383.
- Boehm, M., Yu, J., Reisinger, V., Bečková, M., Eichacker, L.A., Schlodder, E., Komenda, J., and Nixon, P.J. (2012). Subunit composition of CP43-less photosystem II complexes of *Synechocystis* sp. PCC 6803: implications for the assembly and repair of photosystem II. *Philos. Trans. R. Soc. B Biol. Sci.* **367**:3444–3454.
- Diner, B.A., Schlodder, E., Nixon, P.J., Coleman, W.J., Rappaport, F., Lavergne, J., Vermaas, W.F.J., and Chisholm, D.A. (2001). Site-directed mutations at D1-His198 and D2-His197 of photosystem II in *Synechocystis* PCC 6803: sites of primary charge separation and cation and triplet stabilization. *Biochemistry* **40**:9265–9281.
- Dobáková, M., Sobotka, R., Tichý, M., and Komenda, J. (2009). Psb28 protein is involved in the biogenesis of the Photosystem II inner antenna CP47 (PsbB) in the cyanobacterium *Synechocystis* sp. PCC 6803. *Plant Physiol.* **149**:1076–1086.
- Ferreira, K.N., Iverson, T.M., Maghlaoui, K., Barber, J., and Iwata, S. (2004). Architecture of the photosynthetic oxygen-evolving center. *Science* **303**:1831–1838.
- Frank, J., Radermacher, M., Penczek, P., Zhu, J., Li, Y., Ladjadj, M., and Leith, A. (1996). SPIDER and WEB: processing and visualization of images in 3D electron microscopy and related fields. *J. Struct. Biol.* **116**:190–199.
- Funk, C., and Vermaas, W. (1999). A cyanobacterial gene family coding for single-helix proteins resembling part of the light-harvesting proteins from higher plants. *Biochemistry* **38**:9397–9404.
- Guskov, A., Kern, J., Gabdulkhakov, A., Broser, M., Zouni, A., and Saenger, W. (2009). Cyanobacterial photosystem II at 2.9-Å resolution and the role of quinones, lipids, channels and chloride. *Nat. Struct. Mol. Biol.* **16**:334–342.
- Harauz, G., Boekema, E., and van Heel, M. (1988). Statistical image analysis of electron micrographs of ribosomal subunits. *Methods Enzymol.* **164**:35–49.
- He, Q., Dolganov, N., Bjorkman, O., and Grossman, A.R. (2001). The high light-inducible polypeptides in *Synechocystis* PCC6803. Expression and function in high light. *J. Biol. Chem.* **276**:306–314.
- Hernández-Prieto, M.A., Semeniuk, T.A., Giner-Lamia, J., and Futschik, M.E. (2016). The transcriptional landscape of the photosynthetic model cyanobacterium *Synechocystis* sp. PCC6803. *Sci. Rep.* **6**:22168.
- Hollingshead, S., Kopečná, J., Armstrong, D.R., Bučinská, L., Jackson, P.J., Chen, G.E., Dickman, M.J., Williamson, M.P., Sobotka, R., and Hunter, C.N. (2016). Synthesis of chlorophyll-binding proteins in a fully-segregated $\Delta ycf54$ strain of the cyanobacterium *Synechocystis* PCC 6803. *Front. Plant Sci.* **7**:292.
- Janoušek, J., Sobotka, R., Lai, D.H., Flegontov, P., Koník, P., Komenda, J., Ali, S., Prášil, O., Pain, A., Oborník, M., et al. (2013). Split photosystem protein, linear-mapping topology, and growth of structural complexity in the plastid genome of *Chromera velia*. *Mol. Biol. Evol.* **30**:2447–2462.
- Jordan, P., Fromme, P., Witt, H.T., Klukas, O., Saenger, W., and Krauss, N. (2001). Three-dimensional structure of cyanobacterial photosystem I at 2.5 Å resolution. *Nature* **411**:909–917.
- Jung, K.-H., Lee, J., Dardick, C., Seo, Y.-S., Cao, P., Canlas, P., Phetsom, J., Xu, X., Ouyang, S., An, K., et al. (2008). Identification and functional analysis of light-responsive unique genes and gene family members in rice. *PLoS Genet.* **4**:e1000164.
- Kashino, Y., Lauber, W.M., Carroll, J.A., Wang, Q.J., Whitmarsh, J., Satoh, K., and Pakrasi, H.B. (2002). Proteomic analysis of a highly active photosystem II preparation from the cyanobacterium *Synechocystis* sp. PCC 6803 reveals the presence of novel polypeptides. *Biochemistry* **41**:8004–8012.
- Komenda, J., and Barber, J. (1995). Comparison of PsbO and PsbH deletion mutants of *Synechocystis* PCC-6803 indicates that degradation of D1 protein is regulated by the Q(b) site and dependent on protein-synthesis. *Biochemistry* **34**:9625–9631.
- Komenda, J., Reisinger, V., Muller, B.C., Dobáková, M., Granvogl, B., and Eichacker, L.A. (2004). Accumulation of the D2 protein is a key regulatory step for assembly of the photosystem II reaction center complex in *Synechocystis* PCC 6803. *J. Biol. Chem.* **279**:48620–48629.
- Komenda, J., Knoppová, J., Kopečná, J., Sobotka, R., Halada, P., Yu, J.F., Nickelsen, J., Boehm, M., and Nixon, P.J. (2012a). The Psb27 assembly factor binds to the CP43 complex of photosystem II in the cyanobacterium *Synechocystis* sp. PCC 6803. *Plant Physiol.* **158**:476–486.
- Komenda, J., Sobotka, R., and Nixon, P.J. (2012b). Assembling and maintaining the Photosystem II complex in chloroplasts and cyanobacteria. *Curr. Opin. Plant Biol.* **15**:245–251.
- Kopečná, J., Komenda, J., Bučinská, L., and Sobotka, R. (2012). Long-term acclimation of the cyanobacterium *Synechocystis* sp. PCC 6803 to high light is accompanied by an enhanced production of chlorophyll that is preferentially channeled to trimeric Photosystem I. *Plant Physiol.* **160**:2239–2250.
- Kopečná, J., Sobotka, R., and Komenda, J. (2013). Inhibition of chlorophyll biosynthesis at the protochlorophyllide reduction step results in the parallel depletion of Photosystem I and Photosystem II in the cyanobacterium *Synechocystis* PCC 6803. *Planta* **237**:497–508.

- Liu, H.J., Huang, R.Y.C., Chen, J.W., Gross, M.L., and Pakrasi, H.B.** (2011a). Psb27, a transiently associated protein, binds to the chlorophyll binding protein CP43 in photosystem II assembly intermediates. *Proc. Natl. Acad. Sci. USA* **108**:18536–18541.
- Liu, H.J., Roose, J.L., Cameron, J.C., and Pakrasi, H.B.** (2011b). A genetically tagged Psb27 protein allows purification of two consecutive photosystem II (PSII) assembly intermediates in *Synechocystis* 6803, a cyanobacterium. *J. Biol. Chem.* **286**:24865–24871.
- Loll, B., Kern, J., Saenger, W., Zouni, A., and Biesiadka, J.** (2005). Towards complete cofactor arrangement in the 3.0 angstrom resolution structure of photosystem II. *Nature* **438**:1040–1044.
- Mabbitt, P.D., Wilbanks, S.M., and Eaton-Rye, J.J.** (2014). Structure and function of the hydrophilic photosystem II assembly proteins: psb27, Psb28 and Ycf48. *Plant Physiol. Biochem. (Paris)* **81**:96–107.
- Morris, J.N., Crawford, T.S., Jeffs, A., Stockwell, P.A., Eaton-Rye, J.J., and Summerfield, T.C.** (2014). Whole genome re-sequencing of two 'wild-type' strains of the model cyanobacterium *Synechocystis* sp. PCC 6803. *N. Z. J. Bot.* **52**:36–47.
- Nixon, P.J., Michoux, F., Yu, J.F., Boehm, M., and Komenda, J.** (2010). Recent advances in understanding the assembly and repair of photosystem II. *Ann. Bot. (Lond.)* **106**:1–16.
- Nowaczyk, M.M., Hebeler, R., Schlodder, E., Meyer, H.E., Warscheid, B., and Rogner, M.** (2006). Psb27, a cyanobacterial lipoprotein, is involved in the repair cycle of photosystem II. *Plant Cell* **18**:3121–3131.
- Nowaczyk, M.M., Krause, K., Mieseler, M., Sczibilanski, A., Ikeuchi, M., and Rogner, M.** (2012). Deletion of psbJ leads to accumulation of Psb27-Psb28 photosystem II complexes in *Thermosynechococcus elongatus*. *Biochim. Biophys. Acta* **1817**:1339–1345.
- Sakata, S., Mizusawa, N., Kubota-Kawai, H., Sakurai, I., and Wada, H.** (2013). Psb28 is involved in recovery of photosystem II at high temperature in *Synechocystis* sp. PCC 6803. *Biochim. Biophys. Acta* **1827**:50–59.
- Schriek, S., Aguirre-von-Wobeser, E., Nodop, A., Becker, A., Ibelings, B.W., Bok, J., Staiger, D., Matthijs, H.C.P., Pistorius, E.K., and Michel, K.P.** (2008). Transcript profiling indicates that the absence of PsbO affects the coordination of C and N metabolism in *Synechocystis* sp. PCC 6803. *Physiol. Plant* **133**:525–543.
- Sobotka, R., Duerhring, U., Komenda, J., Peter, E., Gardian, Z., Tichý, M., Grimm, B., and Wilde, A.** (2008). Importance of the cyanobacterial GUN4 protein for chlorophyll metabolism and assembly of photosynthetic complexes. *J. Biol. Chem.* **283**:25794–25802.
- Stöckel, J., Jacobs, J.M., Elvitigala, T.R., Liberton, M., Welsh, E.A., Polpitiya, A.D., Gritsenko, M.A., Nicora, C.D., Koppelaar, D.W., Smith, R.D., et al.** (2011). Diurnal rhythms result in significant changes in the cellular protein complement in the cyanobacterium *Cyanothece* 51142. *PLoS One* **6**:e16680.
- Tichý, M., Bečková, M., Kopečná, J., Noda, J., Sobotka, R., and Komenda, J.** (2016). Strain of *Synechocystis* PCC 6803 with aberrant assembly of Photosystem II contains tandem duplication of a large chromosomal region. *Front. Plant Sci.* **7**:648.
- Umena, Y., Kawakami, K., Shen, J.R., and Kamiya, N.** (2011). Crystal structure of oxygen-evolving photosystem II at a resolution of 1.9 Å. *Nature* **473**:55–60.
- Van Heel, M., and Frank, J.** (1981). Use of multivariate statistics in analyzing the images of biological macromolecules. *Ultramicroscopy* **6**:187–194.
- Wellburn, A.R.** (1994). The spectral determination of chlorophyll-a and chlorophyll-b, as well as total carotenoids, using various solvents with spectrophotometers of different resolution. *J. Plant Physiol.* **144**:307–313.
- Wittig, I., Karas, M., and Schagger, H.** (2007). High resolution clear native electrophoresis for in-gel functional assays and fluorescence studies of membrane protein complexes. *Mol. Cell. Proteomics* **6**:1215–1225.
- Yang, Y., Ramelot, T.A., Cort, J.R., Wang, D., Ciccocanti, C., Hamilton, K., Nair, R., Rost, B., Acton, T.B., Xiao, R., et al.** (2011). Solution NMR structure of photosystem II reaction center protein Psb28 from *Synechocystis* sp. strain PCC 6803. *Proteins Struct. Funct. Bioinf.* **79**:340–344.